ChemPubSoc Europe

DOI: 10.1002/cbic.201402602

CHEMBIOCHEM Full Papers

Triplex Crosslinking through Furan Oxidation Requires Perturbation of the Structured Triple-Helix

Ellen Gyssels,[a] Lieselot L. G. Carrette,[a, b] Emma Vercruysse,[a] Kristof Stevens,[a] and Annemieke Madder*[a]

Short oligonucleotides can selectively recognize duplexes by binding in the major groove thereby forming triplexes. Based on the success of our recently developed strategy for furan-based crosslinking in DNA duplexes, we here investigated for the first time the use of the furan-oxidation crosslink methodology for the covalent locking of triplex structures by an interstrand crosslink. It was shown that in a triplex context, although crosslinking yields are surprisingly low (to nonexistent) when targeting fully complementary duplexes, selective crosslinking can be achieved towards mismatched duplex sites at the interface of triplex to duplex structures. We show the promising potential of furan-containing probes for the selective detection of single-stranded regions within nucleic acids containing a variety of structural motifs.

Introduction

Triplex-forming oligonucleotides (TFOs) can recognize a double stranded DNA helix in a highly specific manner.[1–3] Triplexes are formed in vivo, and triplex target sites have been found more abundantly in eukaryotic genes.[4,5] Though the exact roles of triplexes in vivo remain unclear, it is presumed that they are necessary in a range of cellular functions, including transcriptional regulation, DNA repair, post-transcriptional RNA processing, and modification of chromatin.[6] Furthermore, triplex formation is important for long noncoding RNAs that fulfills regulatory roles in gene expression and epigenetics.[7]

It has been demonstrated that TFOs can be applied to actively regulate gene expression by inhibition of transcription.[8–10] TFOs can also be useful in diagnostics, for example to detect single nucleotide polymorphisms (SNP detection).[11] Finally, in the emerging field of DNA nanotechnology, first introduced by Seeman in 1982,[12] straightforward and fast self-assembly of DNA is used to predictably construct a variety of DNA-based motifs.[13] Using triplex formation one can target defined regions on the DNA nanostructure.[14]

In order to irreversibly stabilize the triplex structure one can exploit the formation of interstrand crosslinks (ICL). Covalent locking enables new applications of triplexes and can be used to discover the exact in vivo functions of triplexes. Previously, TFOs linked to DNA-damaging agents have been used to introduce an interstrand crosslink between the TFO and one of the strands of the target duplex. One example is the introduction of thiol functionalities to form a disulfide bridge.[15] Secondly, electrophilic moieties like N-bromoacetyl groups[16,17] or nitrogen mustards[18] are introduced to alkylate the target double-stranded DNA. Another example is the introduction of transplatin to triplex-forming oligonucleotides.[19,20] All these moieties are intrinsically reactive, thus often causing off-target reactions due to poor selectivity. In contrast, some crosslink methodologies can be triggered by external activation to improve selectivity. UV-triggered psoralen-based crosslinking is extensively exploited in the triplex context.[21–25] Upon crosslinking, psoralen-modified TFOs can induce site-specific mutations or recombination.[26] The crosslinking methodology of Sakamoto and co-workers, based on a 3-cyanovinylcarbazole nucleoside, is also triggered by UV irradiation.[27] Alternatively, oxidative activation has been shown to trigger crosslinking with 2-amino-6-vinylpurine-containing oligonucleotides, a methodology developed by Sasaki and co-workers,[28,29] and has been used by Greenberg and co-workers to allow activation of and crosslinking with phenylselenyl-modified pyrimidines.[30]

In the context of externally activated crosslink methodologies, we recently achieved selective interstrand crosslinking in duplex DNA by introducing furan-modified nucleosides.[31–35] This site-selective and high-yielding crosslink methodology was inspired by the natural toxicity of furan.[31–38] Furan is toxic, and is classified as possibly carcinogenic by the IARC.[39,40] It is oxidized by cytochrome P450 to its metabolite *cis*-but-2-ene-1,4-dial,[41] which is known to react with nucleobases.[42] Furan introduction into oligonucleotides is relatively straightforward, as various furan derivatives are commercially available, and the small aromatic moiety is stable under both nucleoside and oligonucleotide synthesis conditions. After hybridization of the furan-modified oligonucleotide with its complement, furan can selectively be oxidized to a reactive keto-enal functionality that

[a] E. Gyssels, Dr. L. L. G. Carrette, E. Vercruysse, Dr. K. Stevens, Prof. Dr. A. Madder
Organic and Biomimetic Chemistry Research Group
Department of Organic and Macromolecular Chemistry, Ghent University
Krijgslaan 281, S4, 9000 Gent (Belgium)
E-mail: annemieke.madder@ugent.be

[b] Dr. L. L. G. Carrette
Present address: Lee Laboratory, Department of Molecular Biology/Genetics
Massachusetts General Hospital/Harvard Medical School
185 Cambridge Street, Simches Research Ctr., Boston, MA 02114 (USA)

Supporting information for this article is available on the WWW under http://dx.doi.org/10.1002/cbic.201402602.

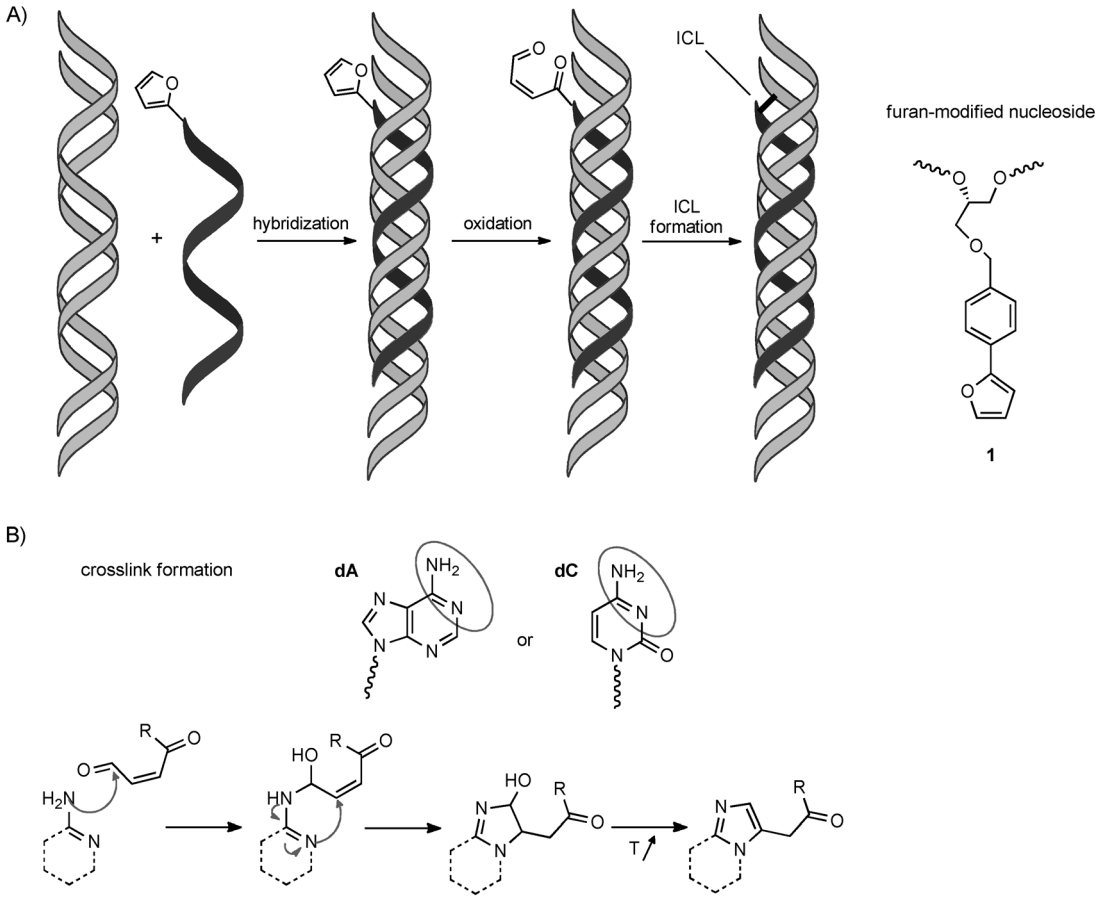

Scheme 1. A) Furan oxidation crosslink methodology in a triplex context. B) Mechanism of nucleic acid crosslink formation. The exocyclic amine of cytidine or adenosine attacks the aldehyde of the oxidized furan moiety to form a stable crosslink.

is susceptible to nucleophilic attack (Scheme 1 B). The exocyclic amines of A and C opposite the modified nucleoside react with the electrophilic keto-enal to form a clean interstrand crosslink within the duplex in high yield.[33] The oxidation conditions can be very mild (red light irradiation to generate singlet oxygen), thus rendering this furan crosslink strategy broadly applicable.[36]

We now explored for the first time the usefulness and application potential of the furan crosslink methodology in a triplex context (Scheme 1 A) by targeting double-stranded rather than single-stranded DNA. A short oligonucleotide can bind in the major groove of a purine-rich part of a duplex by Hoogsteen hydrogen bonding. Two possible motifs exist: a parallel triplex, and an anti-parallel triplex (Scheme 2). In the anti-parallel triplex motif, the TFO, consisting of G, A, and T, is oriented antiparallel to the purine rich strand of the duplex. G-rich TFOs can also form highly stable aggregates such as G-quadruplexes.[43,44] Parallel triplexes on the other hand, are formed when the TFO is oriented parallel to the purine-rich strand of the duplex. In this case cytosine protonation (C^+) within the TFO is necessary to allow formation of two Hoogsteen hydrogen bonds with guanosine, thus limiting this triplex formation to slightly acidic conditions (pH 5). However, this can be solved by using synthetically modified nucleotides in the TFO to target natural duplexes.[45,46] We thus decided to study our furan crosslink method in a parallel triplex context. Also, previous strategies for triplex crosslinking were mostly based on parallel triplexes.[19–21,24,25,28,30]

Results and Discussion

Synthesis of furan-modified triplex-forming oligonucleotides

The furan-modified acyclic nucleoside analogue **2** was synthesized, transformed into its phosphoramidite, and incorporated centrally in an oligonucleotide by standard oligonucleotide synthesis procedures (Scheme 3 A), as previously described.[38] Additionally, to allow incorporation of the furan-modified nucleoside at the 3′-end of the TFO, **2** was directly attached to controlled pore glass (CPG; **5**; Scheme 3, route B), which was subsequently used in standard oligonucleotide synthesis.

Three different furan-modified TFOs were synthesized (Figure 1 A). TFO1 had the furan moiety internally in the sequence and can be combined with duplex ON1/ON2 to crosslink to an AT base pair or with duplex ON3/ON4 to crosslink to a GC base pair. In TFO2 and TFO3 the furan moiety was incorporated at the 3′-ends to crosslink to AT and GC base pairs, respectively, in the complementary duplex ON1/ON2.

The formed triplexes were detected by the observation of biphasic melting during melting temperature measurements.

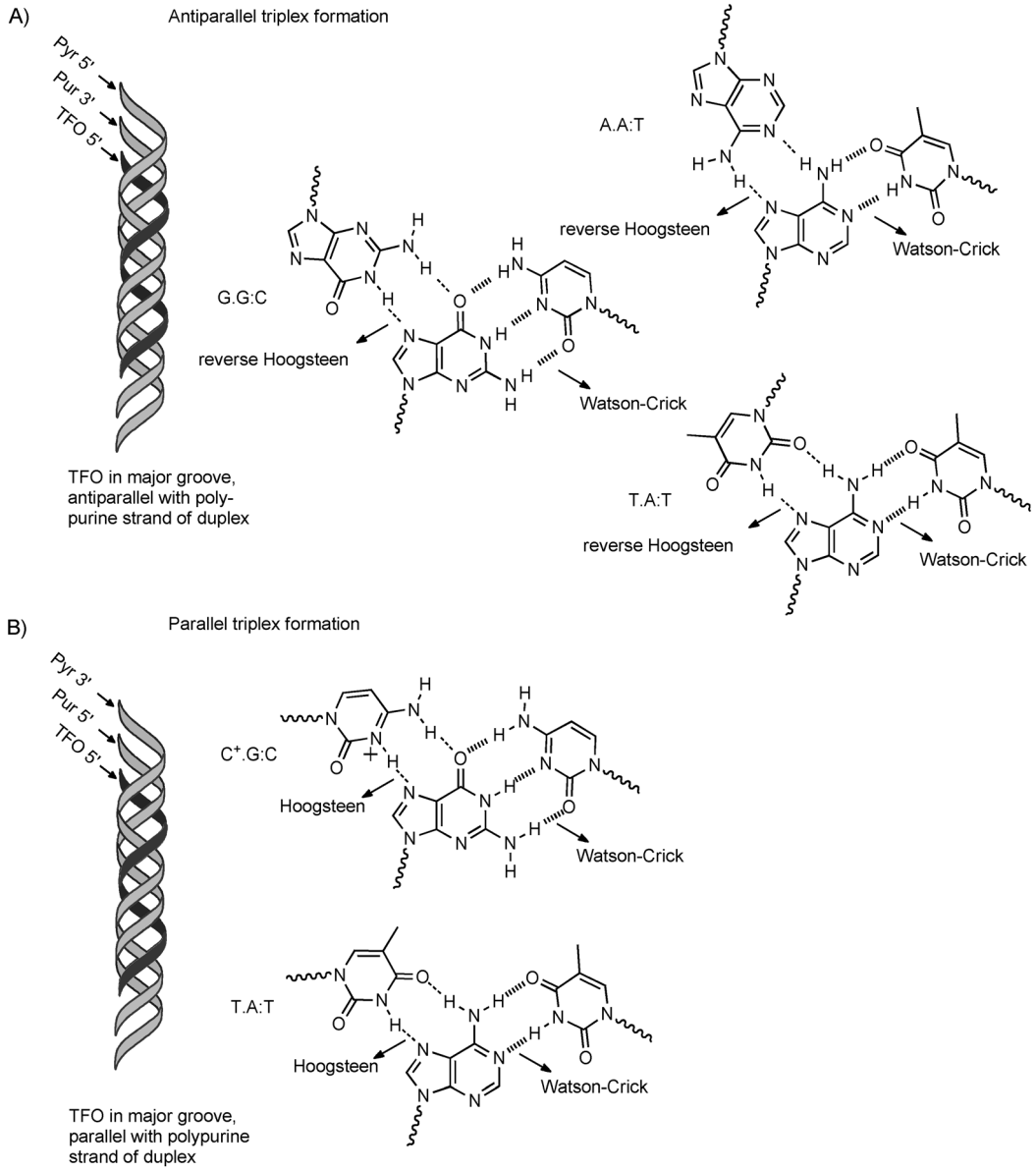

Scheme 2. Triplex formation. A) Anti-parallel triplex formation with base triplets (A·A:T; G·G:C and T·A:T). B) Parallel triplex formation with base triplets (C^+·G:C and T·A:T)

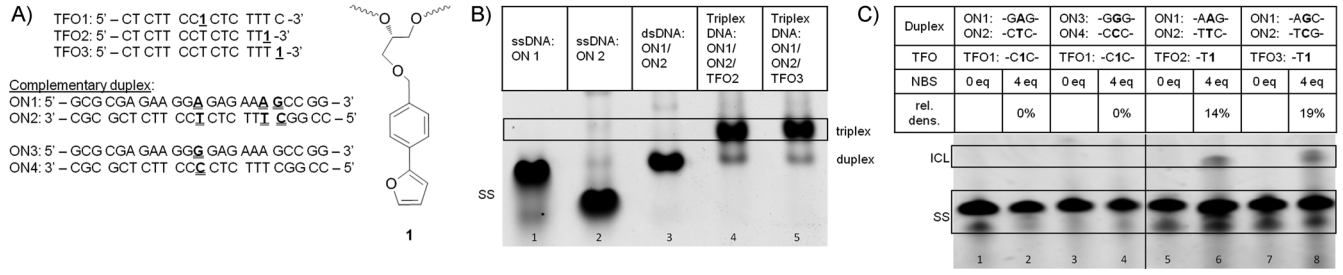

Figure 1. A) Furan-modified TFOs and their target duplexes. The furan moiety is introduced by incorporation of acyclic building block **1** either internally (TFO1) or at the 3′-end of the sequence (TFO2 and TFO3). Two complementary target duplexes are used: ON1/ON2 has an AT base pair opposite the internal furan of TFO1; an AT base pair opposite the external furan in TFO2; or a GC base pair opposite the external furan of TFO3. Duplex ON3/ON4 has a GC base pair opposite the internal furan of TFO1. B) Non-denaturing PAGE analysis of single strands and duplex and triplex structures. Electrophoresis was performed on a 16% acrylamide gel in TAE buffer (pH 5). C) Denaturing PAGE analysis of triplex crosslinking with furan incorporated internally (lane 1–4) or at the 3′-end (lane 5–8). Odd lanes are the references before oxidation; even lanes represent reaction mixtures after oxidation with 4 equiv of NBS. Electrophoresis was performed in TBE buffer on a 16% acrylamide gel containing 8 M urea. Within each lane, the relative density of the crosslink product is determined in comparison to the total density of the single strands and the crosslink product.

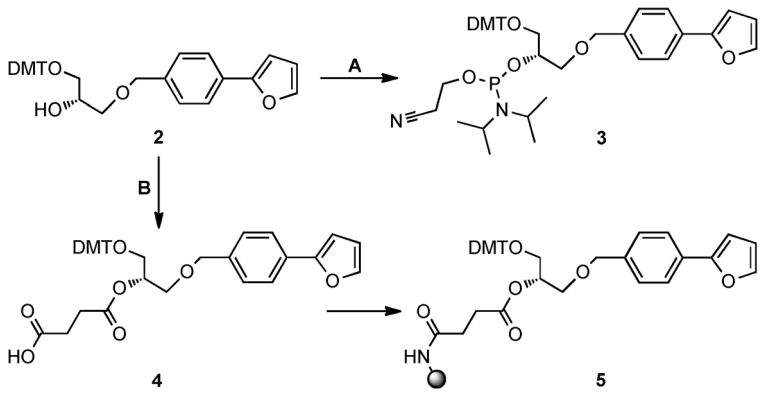

Scheme 3. DMT-protected furan-modified acyclic nucleoside **2** and its transformation into phosphoramidite **3** for internal incorporation (A), or onto solid supported **5** for 3′-incorporation (B). A) 2-Cyanoethyl *N*,*N*,*N*′,*N*′-tetraisopropylphosphordiamidite, *N*,*N*-diisopropyl ammonium tetrazolide, CH_2Cl_2, 48 h, 0 °C, 79%; B) i: succinic anhydride, Et_3N, CH_2Cl_2, RT, 4 h, 71%; ii: long-chain alkylamine controlled-pore glass, 1-hydroxy benzotriazole, *N*,*N*-diisopropylcarbodiimide, ACN, pyridine, RT, overnight.

The melting temperature of the natural 23-mer duplex ON1/ON2 was 72.1 °C. When TFO2 was added, the triplex melted at 58.9 °C, whereas the duplex melting temperature remained almost unchanged (Section 5 in the Supporting Information). Triplex formation with the modified TFOs was further confirmed by native polyacrylamide gel electrophoresis (PAGE), by the observation of a shifted band for triplex species (Figure 1 B).

Crosslink formation in triplex DNA

We then investigated the crosslinking propensity of the furan-modified TFOs towards dsDNA. After hybridization to the target duplex, selective oxidation of the furan moiety was achieved through the addition of *n*-bromo succinimide (NBS; Section 2 in the Supporting Information). Four equivalents of NBS were added, at a rate of one equivalent every 15 min. First, crosslink reactions were performed for TFO1 (internal furan). The absence of a formed product in both HPLC analysis (Section 6.1 in the Supporting Information) and denaturing PAGE (Figure 1 C, lanes 1–4) showed that crosslinking had not occurred. In view of the high yield typically obtained with the furan oxidation methodology in a duplex context, the lack of reactivity of the TFO for crosslinking to the target duplex seemed rather surprising. As triplex formation had been demonstrated (vide supra), lack of proximity between the oxidized furan and the target DNA was thus unlikely to have been the problem.

Interestingly, with TFO2 (furan at the 3′-end), crosslinking did occur. This was evident in PAGE analysis by the formation of a new product eluting at a higher position (ICL; Figure 1 C) than the single-stranded sequences (SS; Figure 1 C lanes 5–8). Still, a substantially lower amount of crosslinked species was observed compared to what was generally obtained in the duplex context. The formed product was analyzed and confirmed to be the crosslinked species by mass analysis (Section 7 in the Supporting Information). The crosslink was formed between the TFO and the polypyrimidine strand of the duplex (ON2), as determined by HPLC analysis (Section 6.1 in the Supporting Information) and further confirmed by mass analysis. (Calculated mass crosslink product ON2-TFO2: 10992.83; ESI-MS: 10992.46. Calculated mass crosslink product ON2-TFO3: 11296.88; ESI-MS: 11294.96; Section 7 in the Supporting Information). In addition, a negligible amount of brominated product, a known side product, was formed (Section 2 in the Supporting Information).[33]

The modified base in TFO2 was targeted against an AT base pair in the ON1/ON2 duplex. As the target thymine in ON2 does not contain the necessary exocylic amine nucleophile to perform the nucleophilic attack, we assume the crosslink was formed with the neighboring cytosine. In TFO3, the furan-modified base targets a GC base pair and can thus nicely crosslink to the complementary C base in ON2.

In an effort to explain these unexpected results, previous reports on triplex crosslink strategies were analyzed in more detail. Though some other methodologies allow crosslinking at an internal position of the triplex (e.g., transplatin[20] or 2-amino-6-vinylpurine[29] mediated crosslinking), most of the reported triplex crosslinking took place at the 5′- or 3′-end of the TFO.[15–18] Interestingly, for psoralen-mediated crosslinking, specific intercalation at the duplex to triplex junction was exploited.[24,47]

In furan-modified triplexes formed with TFO2 and TFO3, the furan moiety is at the triplex–duplex junction. One can thus reason that crosslinking is more successful there, as at the duplex to triplex transition point local distortion of the structure enables the involvement of the target nucleobase in Watson–Crick base-pair formation to be weakened thus allowing this nucleobase to attack the formed reactive enal. Therefore it seems that in order to obtain high crosslink yields, base pairing in the target duplex needs to be locally destabilized. Indeed, in previous duplex crosslinking studies, single-stranded rather than fully base-paired double-stranded DNA was targeted. In that case, the furan moiety within the modified strand targeted a base on the complementary strand, which is not involved in Watson–Crick base pairing. In addition, in all previous studies a positive correlation between crosslink yield and degree of duplex destabilization (caused by the furan-modified nucleoside incorporation) was found; this further underscores the importance of nucleobase availability.

To further illustrate this important difference between duplex and triplex crosslinking, TFO3 was combined with its complement ON5 for verification of its intrinsic duplex crosslinking capability in the current context.

Though duplex crosslinking with furan containing building block **1** has previously been demonstrated,[37] it was not investigated with this type of polypyrimidine sequences. However, as expected, TFO1 and TFO3, when targeted to a freely available base in the complementary strand, also allowed clean and efficient crosslinking, as observed by PAGE and HPLC.

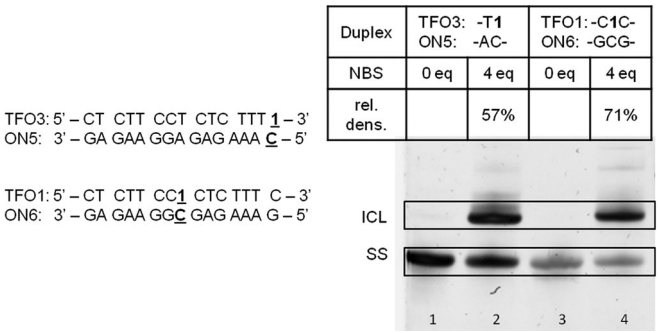

Figure 2. PAGE analysis of duplex crosslinking. Odd lanes are the references before oxidation; even lanes contain the reaction mixture after oxidation with 4 equiv of NBS. The furan at the 3′-end of the oligo targets an opposite C (lanes 1 and 2; TFO3/ON5); the internal furan targets an opposite C (lanes 3 and 4; TFO1/ON6). Electrophoresis was performed in TBE buffer on a 16% acrylamide gel containing 8 M urea. Within each lane, the relative density of the crosslink product is determined in comparison to the total density of the single strands and the crosslink product.

(Figure 2) The relative density[1] of the crosslink product based on PAGE was 57% for ON5/TFO3 and 71% for ON6/TFO1. The fact that duplex crosslink yields are lower when the furan moiety is incorporated at the 3′-end (TFO3/ON5) can be explained by the decreased proximity between the oxidized furan and the target base as a result of end-fraying of the duplex. These results confirmed the intrinsic crosslink capability of **1**.

Further proof of the hypothesis that nucleobase availability is of importance for efficient crosslinking was obtained in parallel studies where furan-modified DNA binding peptides were targeted against a double-stranded DNA helix (unpublished results, see also Section 8 in the Supporting Information). Though the employed dipodal peptides (derived from the DNA-binding sequence of the GCN4 transcription factor) were shown to bind the target DNA duplex, crosslinking of the oxidized furan moiety within the peptide to one of the nucleobases of the target duplex could not be achieved. In contrast, crosslinking from a furan-modified DNA strand within the duplex to the lysine side chain functionality of bound peptides was successful.[38]

Improved triplex crosslinking by disturbing the duplex

Building on these new insights, an increase in the yield of triplex crosslinking was attempted by disturbing the target DNA helix while keeping the triplex formation. For this, in a first test, the reactions were performed at higher temperatures. It is clear from denaturing gel electrophoresis experiments that crosslink yield first increased with temperature (from a relative density of 9% to a maximum of 14% at 45 °C) and then decreased (Figure 3B). This trend can be explained by thermal disturbance of the triplex; this first occurs locally at the site of the modified nucleoside, thus allowing better crosslinking because of the increased nucleobase availability, until the triplex structure melts (at 60.5 °C).

Next, crosslinking was tested against mismatched duplexes in which a non-Watson–Crick base pair was present opposite furan. TFO1 (furan in the middle of the sequence) was combined with AC- (ON1/ON4), CC- (ON7/ON4), and TC- (ON8/ON4) mismatches (Figure 3C, lanes 3–8). No crosslink product was formed in any of these triplexes. The mismatch effect on its own does not sufficiently perturb the duplex to allow crosslinking when using TFO1 (internally modified). TFO3 (furan at the 3′-end) was hybridized both with a CC-mismatch (ON9/ON2) and a TC-mismatch (ON10/ON2). PAGE analysis indeed showed that significant improvements in crosslinking were obtained by selective furan oxidation of these TFO mismatched duplex complexes at room temperature (Figure 3C lanes 9–12). The relative density of the crosslink product was shown to increase to 33% in the case of the CC-mismatch opposite furan. The combination of the mismatch effect and the perturbation at the triplex to duplex junction ensured the required nucleophile availability, thus resulting in a higher yield of crosslink product.

Selective crosslinking to single-stranded regions

Because of the clearly observed preference of crosslinking to single strands and the unavailability of the required nucleophiles in double-stranded regions, the methodology should thus allow selective detection of single-stranded regions in a mixed single- and double-stranded nucleic acid structure. This type of selective crosslinking to single-stranded regions may be used to reveal the secondary structure in higher-order RNA sequences or to identify single-stranded regions in DNA. Identification of single-stranded regions is of interest because these regions are important in transcription[48] and in RNA interactions.[49] Furthermore, clustered mutations are generated in long single-stranded DNA regions in human cancers.[50] Single-stranded regions are often detected by specific DNA-binding proteins; for example, S1 nuclease specifically cleaves DNA in its single-stranded form.[51] Potassium permanganate is also used to detect single-stranded regions, by oxidation of the pyrimidines, thus causing cleavage of the backbone.[52,53] However, the furan crosslink strategy offers a detection method without cleavage of the structure.

This potential was illustrated in a competition experiment in which the TFO had both a dsDNA and ssDNA target (Figure 4). Duplex ON11/ON4 has a double-stranded and a single-stranded region, both of which are complementary to TFO1. Upon oxidative treatment of the complex ON11/ON4/TFO1, only the ON11–TFO1 crosslink product appeared in denaturing PAGE analysis (lane 3); this is the product of crosslinking to the single-stranded region. Crosslink product ON4–TFO1, which would be formed upon triplex crosslinking as ON4 is the polypyrimidine strand, did not appear in the PAGE analysis. Moreover, changing the sequence of the single-stranded region by mismatching the four surrounding base pairs aside the cross-

[1] *The relative density of the spots on the gels cannot be used for calculating yields, as the gels were stained with GelRed, which has a different sensitivity for single-stranded versus double-stranded versus triplex species. We here only refer to these values in a comparative way, each time comparing relative densities between complexes of equal nature and sensitivity for GelRed.*

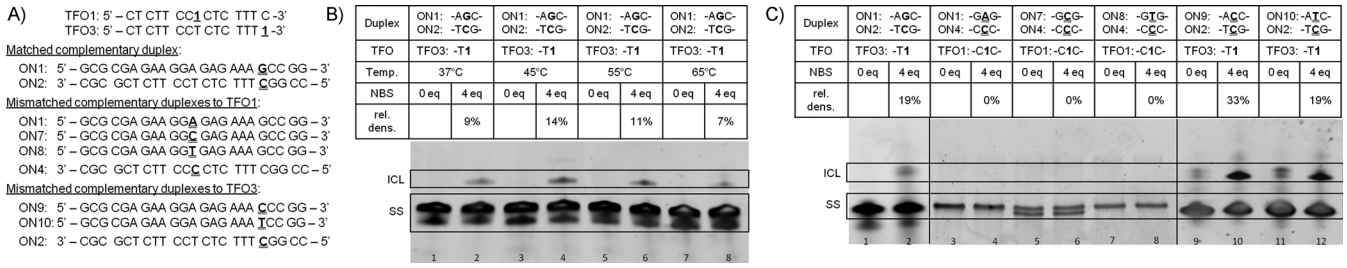

Figure 3. A) Sequences of the matched and mismatched triplexes. B) PAGE analysis of triplex crosslinking (ON1/ON2/TFO3) at different temperatures. C) PAGE analysis of triplex crosslinking with the furan-modified TFO3, when targeting a matched duplex (ON1/ON2) and mismatched duplexes (ON9/ON2 or ON10/ON2), and internally modified TFO1 targeting mismatched duplexes (ON1/ON4, ON7/ON4, or ON8/ON4). Odd lanes contain the references before oxidation; even lanes contain the reaction mixture after oxidation with 4 equiv of NBS. Electrophoresis was performed in TBE buffer on a 16% acrylamide gel containing 8 M urea. Within each lane, the relative density of the crosslink product is determined in comparison to the total density of the single strands and the crosslink product. As can be seen in lanes 9 and 11 of C), there is an impurity already at 0 equiv of NBS. The relative density for crosslink products in lanes 10 and 12 are therefore reduced with this impurity.

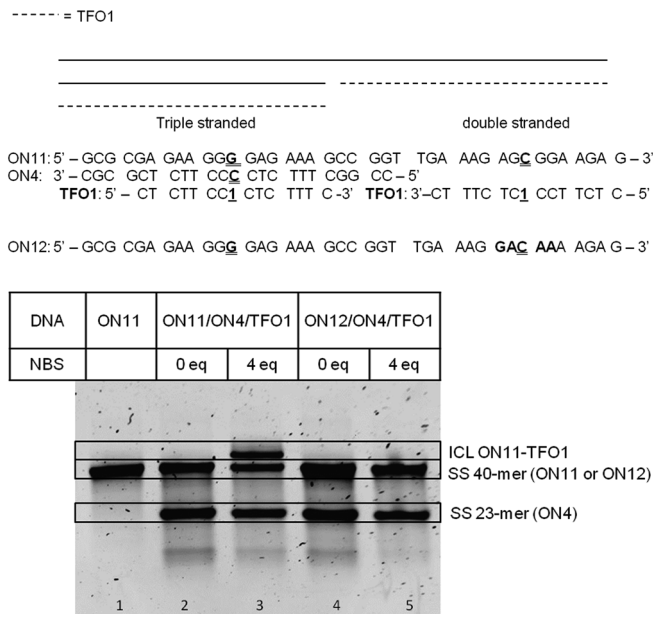

Figure 4. PAGE analysis of crosslinking with the furan-modified TFO1 targeting a double-stranded region (ON11/ON4) and a single-stranded region (ON11). ON12 was used as a control, by forming a complementary double-stranded region to TFO1, but in the single-stranded region four mismatches are introduced, thus making this single-stranded region not complementary to TFO1. Lane 1: single stranded 40-mer ON11; lanes 2 and 4: crosslink reaction before addition of NBS; lanes 3 and 5: reaction mixture after oxidation with 4 equiv of NBS. Electrophoresis was performed in TBE buffer on a 16% acrylamide gel containing 8 M urea.

link site (ON12) caused loss of binding by TFO1 to that single-stranded target. As seen in PAGE analysis (lane 5), no crosslink product was formed upon oxidative treatment of ON12/ON4/TFO1.

Furan oxidation crosslinking with an internally modified furan oligonucleotide thus offers a very specific methodology that requires the fulfillment of two conditions for the formation of crosslinked species: the target should be complementary and single stranded. Though this hampers the application of the methodology for triplex crosslinking, it is clear from the current studies that this stringency can be exploited for the study of nucleic acid structures.

Conclusion

In this work we illustrate that, rather unexpectedly, the furan oxidation crosslinking methodology is not applicable for triplex crosslinking when using fully matched duplexes as the target. By experiments with the triplex to duplex junction, evidence is provided that at higher temperatures and for a mismatched target duplex, nucleophile availability is prerequisite for crosslinking in high yield. The necessary nucleophile should not be involved in Watson–Crick base pairing. By taking advantage of the inherent stringency of this methodology, we were able to selectively crosslink to a single-stranded target site within a target containing a combination of single- and double-stranded target regions. This methodology could therefore offer promising perspectives in selective mismatch detection or the identification of single-stranded regions within nucleic acid sequences.

Experimental Section

Materials and methods for chemical synthesis: All solvents and chemical reagents were purchased from Sigma–Aldrich and were at the highest purity available. ^{1}H NMR and ^{13}C NMR spectra were recorded at room temperature on an Avance 300 or a DRX 500 spectrometer (Bruker). Chemical shifts are reported in parts per million relative to the residual solvent peak. RP-HPLC-MS data were recorded at 35 °C on an 1100 series LC/MS system (Agilent Technologies) equipped with a Luna C18 column (250×4.6 mm, 5 μm; Phenomenex). The solvent system was NH_4OAc (5 mM) in water (A) and MeCN (B). The gradient was 0–100% B over 15 min.

Synthesis of furan-modified building blocks-: The furan-modified and protected nucleoside analogue (**2**) and the phosphoramidite (**3**) were synthesized as previously described.[38]

(*S*)-4-(1-(Bis(4-methoxyphenyl)(phenyl)methoxy)-3-(4-(furan-2-yl)benzyloxy)propane-2-yloxy-4-oxobutanic acid (4): Compound **2** (1 equiv, 0.1 mmol, 54 mg) was dissolved in CH_2Cl_2 (1 mL); succinimate anhydride (1.5 equiv; 0.15 mmol; 15 mg) and triethylamine (3 equiv; 0.29 mmol; 0.04 mL) were added, and the reaction mixture was stirred for 4 h. The reaction mixture was washed with citric acid (4%, 2 mL). Compound **4** was obtained in sufficient purity for coupling on controlled-pore glass (CPG). IR (cm^{-1}): $\tilde{\nu}$ = 3462.5 (w), 2930.6 (m), 2358.9 (m), 2385.9 (m), 1607.0 (m), 1578.9

(m), 1508.0 (s), 1460.1 (m), 1444.6 (m), 1300.6 (m), 1250.9 (s), 1175.8 (s), 1152.7 (m), 1077.3 (s), 1033.5 (s), 1010.7 (m), 828.1 (s), 801.4 (m), 7359 (m), 702.2 (m); LC-MS: *m/z*: 651.25 $[\mathbf{4}+H]^+$ (t_R = 4.3 min), 551.24 $[\mathbf{2}+H]^+$ (t_R = 10.5 min).

Immobilization of 4 on CPG (5): CPG (517 mg), MeCN (2.24 mL), pyridine (0.11 mL), 1-hydroxybenzotriazole (0.27 equiv; 0.02 mmol; 2.3 mg), and *N*,*N*-diisopropylcarbodiimide (2.7 equiv; 0.17 mmol; 26 μL) were stirred for 30 min. Compound **4** was dissolved in a minimum of MeCN and added to the reaction mixture, which was stirred overnight. The reaction mixture was filtered, and the solid phase was washed with MeOH and CH_2Cl_2. The remaining free amines were acetylated with cap A (THF/2.6-lutidine/acetic acid 8:1:1, 5 mL) and cap B (1-methylimidazole (10%) in THF, 5 mL), then the reaction mixture was stirred for 1 h and washed with MeOH and CH_2Cl_2 and dried.

Oligonucleotides: Non-modified DNA sequences were purchased from Eurogentec (Seraing, Belgium).

Reagents for DNA synthesis were obtained from Glen Research (Sterling, VA). All RP-HPLC experiments were recorded on a 1200 system (Agilent Technologies) equipped with a Clarity 110 Å C18 column (250×4.6 mm, 5 μm; Phenomenex) or an Aeris Widepore column (150×4.6 mm, 3.6 μm; Phenomenex) at 60 °C in TEAA (0.1 M, with MeCN (5%)) and MeCN as mobile phases (linear gradient: 0–30% MeCN over 15 or 30 min). MALDI-TOF spectra of oligonucleotides were recorded on a Voyager DE-STR MALDI-TOF (Applied Biosytems) in positive mode. The matrix was a mixture of 3-hydroxypicolinic acid (17 mg in 100 μL ultrapure water) and ammonium citrate (10 mg in 40 μL ultrapure water and 50 μL MeCN). The samples were desalted by addition of DOWEX beads, which were thoroughly rinsed with water before use. A desalted sample (0.35 μL) was spotted on the MALDI plate. ESI-MS spectra of oligonucleotides were recorded on a quadrupole ion trap LC mass spectrometer (Thermo Scientific) with electrospray ionization. Data were acquired in the negative ionization mode. The mass spectra were deconvoluted with LC/MSD ChemStation software (version A.08014; Agilent Technologies).

Synthesis of modified DNA: All oligonucleotides were synthesized with the last nucleoside still DMT-protected (DMT-on) in an ABI 394 DNA synthesizer at 1 μmol scale. A standard synthesis protocol was used except for coupling of the modified residues. The synthesis column was removed from the DNA synthesizer for the introduction of the modified residues. For these manual couplings, the phosphoramidite (60 mM) in acetonitrile and DCI (100 mM) in acetonitrile were dried on molecular sieves for about 10 min. Small portions of the phosphoramidite solution (0.4 mL) and the DCI solution (0.5 mL) were then alternately passed over the reaction column for 20 min. The column was reinstalled on the DNA synthesizer, and automated synthesis was resumed. Oligonucleotides were cleaved from the solid support and deprotected by incubation at 55 °C overnight in concentrated aqueous ammonia. The synthesized DMT-oligonucleotides were deprotected and purified on SEP-PAK C18 cartridges (Waters).

UV measurements: Oligonucleotides concentrations were measured with a DropSense96 UV/VIS droplet reader (Trinean, Gentbrugge, Belgium). Thermal denaturation experiments were recorded on a Varian Cary 300 Bio instrument (Agilent Technologies) equipped with a six-cell thermostatted cell holder. Melting curves were monitored at 260 nm, with a heating rate of 0.3 °C min^{-1}. The NaOAc/HOAc buffer (10 mM, pH 5) contained NaCl (100 mM) and $MgCl_2$ (2 mM). Duplex concentration was 1 μM and TFO concentration was 1.5 μM. Melting temperatures were calculated from the first derivative of the heating curves (Cary 300 Bio software).

Crosslink reactions: The modified TFO (0.03 mM, 1.5 nmol) was mixed with its complementary duplex (0.02 mM, 1 nmol) in NaOAc/HOAc buffer (10 mM, pH 5, 50 μL) containing NaCl (100 mM) and $MgCl_2$ (2 mM). The triplexes were slowly annealed by reducing the temperature from 95 °C to room temperature. During the subsequent crosslink reaction the temperature was kept constant in an Eppendorf thermomixer comfort at 25 °C (unless otherwise mentioned, see temperature study Figure 3B). A stock solution of NBS (1.5 nmol, 2 μL) was freshly prepared, and to start the reaction, NBS (1 equiv, 1.5 nmol) of was added. This was repeated every 15 min until complete disappearance of the modified oligonucleotide. The reactions were monitored by HPLC. For duplex crosslinking and the competition experiment (crosslinking with sequence containing single- and double-stranded regions, see Figure 4) the same procedure was used, but at pH 7 and without $MgCl_2$. TFO (1 nmol) was used for duplex crosslinking, and TFO (2 nmol) was used in the competition experiment.

For mass analysis of the crosslink product, the crosslinking reaction was performed on a larger scale: duplex (20 nmol) and TFO (30 nmol). The concentrations were the same as in small-scale experiments. The crosslinked product was purified by fraction collection on RP-HPLC and analyzed with ESI-MS.

Gel electrophoresis experiments: A 16% polyacrylamide gel (acrylamide/bisacrylamide 37.5:1) with Tris/acetate/EDTA (TAE; 1×) buffer (pH 5) was used for native PAGE. For denaturing PAGE, urea (8 M) was added to a 16% polyacrylamide gel (acrylamide/bisacrylamide 37.5:1) with Tris/Borat/EDTA (TBE; 1×) buffer. The temperature of the gel was maintained at 25 °with an F12-C circulator (Julabo, Seelbach, German). The power supply was a Consort EV202. Gels were stained with GelRed (VWR), and pictures were taken with an Autochemi imaging system (UVP, Upland, CA). The total density of the spots was calculated with UVP software. Relative density was calculated as the total density of the crosslink product divided by the sum of the total densities of all the products in that lane.

Acknowledgements

E.G. is indebted to the Agency for Innovation by Science and Technology in Flanders (IWT). L.L.G.C. would like to thank the Research Foundation–Flanders (FWO) for an aspirant and postdoc position and the Belgian American Educational Foundation (BAEF) and the Gustave Boël Sofina Foundation for support. We would also like to thank the European Union's Seventh Framework Programme (FP7/2007–2013)/Marie Curie ITN Grant Agreement No. 316975.

Keywords: DNA structures · furan oxidation · nucleic acid crosslinking · nucleosides · triplex DNA

[1] G. Felsenfeld, D. R. Davies, A. Rich, *J. Am. Chem. Soc.* **1957**, *79*, 2023–2024.
[2] M. D. Frank-Kamenetskii, S. M. Mirkin, *Annu. Rev. Biochem.* **1995**, *64*, 65–95.
[3] N. T. Thuong, C. Hélène, *Angew. Chem. Int. Ed. Engl.* **1993**, *32*, 666–690; *Angew. Chem.* **1993**, *105*, 697-723.
[4] G. P. Schroth, P. S. Ho, *Nucleic Acids Res.* **1995**, *23*, 1977–1983.
[5] M. J. Behe, *Nucleic Acids Res.* **1995**, *23*, 689–695.

[6] F. A. Buske, J. S. Mattick, T. L. Bailey, *RNA Biol.* **2011**, *8*, 427 – 439.
[7] I. Martianov, A. Ramadass, A. Serra Barros, N. Chow, A. Akoulitchev, *Nature* **2007**, *445*, 666 – 670.
[8] S. Sasaki, *Eur. J. Pharm. Sci.* **2001**, *13*, 43 – 51.
[9] P. Saraswat, R. R. Soni, A. Bhandari, B. P. Nagori, *Indian J. Pharm. Sci.* **2009**, *71*, 488 – 498.
[10] Y. Fichou, C. Férec, *Trends Biotechnol.* **2006**, *24*, 563 – 570.
[11] J. I. Daksis, G. H. Erikson, *PLoS One* **2007**, *2*, e305.
[12] N. C. Seeman, *J. Theor. Biol.* **1982**, *99*, 237 – 247.
[13] B. Saccà, C. M. Niemeyer, *Angew. Chem. Int. Ed.* **2012**, *51*, 58 – 66; *Angew. Chem.* **2012**, *124*, 60 – 69.
[14] D. A. Rusling, I. S. Nandhakumar, T. Brown, K. R. Fox, *Chem. Commun.* **2012**, *48*, 9592 – 9594.
[15] S. E. Osborne, R. J. Cain, G. D. Glick, *J. Am. Chem. Soc.* **1997**, *119*, 1171 – 1182.
[16] K. B. Grant, P. B. Dervan, *Biochemistry* **1996**, *35*, 12313 – 12319.
[17] M. J. Taylor, P. B. Dervan, *Bioconjugate Chem.* **1997**, *8*, 354 – 364.
[18] M. W. Reed, E. A. Lukhtanov, V. Gorn, I. Kutyavin, A. Gall, A. Wald, R. B. Meyer, *Bioconjugate Chem.* **1998**, *9*, 64 – 71.
[19] M. A. Campbell, P. S. Miller, *Bioconjugate Chem.* **2009**, *20*, 2222 – 2230.
[20] E. Bernal-Méndez, J.-s. Sun, F. González-Vílchez, M. Leng, *New J. Chem.* **1998**, *22*, 1479 – 1483.
[21] H. Li, V. J. Broughton-Head, G. Peng, V. E. C. Powers, M. J. Ovens, K. R. Fox, T. Brown, *Bioconjugate Chem.* **2006**, *17*, 1561 – 1567.
[22] Y. Liu, R. S. Nairn, K. M. Vasquez, *Nucleic Acids Res.* **2009**, *37*, 6378 – 6388.
[23] J. Song, Z. Intody, M. Li, J. H. Wilson, *Gene* **2004**, *324*, 183 – 190.
[24] M. Takasugi, A. Guendouz, M. Chassignol, J. L. Decout, J. Lhomme, N. T. Thuong, C. Hélène, *Proc. Natl. Acad. Sci. USA* **1991**, *88*, 5602 – 5606.
[25] C. Le Breton, M. Hennion, P. B. Arimondo, O. Hyrien, *PLoS One* **2011**, *6*, e18554.
[26] K. M. Vasquez, G. Wang, P. A. Havre, P. M. Glazer, *Nucleic Acids Res.* **1999**, *27*, 1176 – 1181.
[27] K. Fujimoto, H. Yoshinaga, Y. Yoshio, T. Sakamoto, *Org. Biomol. Chem.* **2013**, *11*, 5065 – 5068.
[28] F. Nagatsugi, S. Sasaki, *Biol. Pharm. Bull.* **2004**, *27*, 463 – 467.
[29] F. Nagatsugi, T. Kawasaki, D. Usui, M. Maeda, S. Sasaki, *J. Am. Chem. Soc.* **1999**, *121*, 6753 – 6754.
[30] X. Peng, I. S. Hong, H. Li, M. M. Seidman, M. M. Greenberg, *J. Am. Chem. Soc.* **2008**, *130*, 10299 – 10306.
[31] S. Halila, T. Velasco, P. De Clercq, A. Madder, *Chem. Commun.* **2005**, 936 – 938.
[32] K. Stevens, A. Madder, *Nucleic Acids Res.* **2009**, *37*, 1555 – 1565.
[33] K. Stevens, D. D. Claeys, S. Catak, S. Figaroli, M. Hocek, J. M. Tromp, S. Schürch, V. Van Speybroeck, A. Madder, *Chem. Eur. J.* **2011**, *17*, 6940 – 6953.
[34] A. M. Jawalekar, M. Op de Beeck, F. L. van Delft, A. Madder, *Chem. Commun.* **2011**, *47*, 2796 – 2798.
[35] M. Op de Beeck, A. Madder, *J. Am. Chem. Soc.* **2011**, *133*, 796 – 807.
[36] M. Op de Beeck, A. Madder, *J. Am. Chem. Soc.* **2012**, *134*, 10737 – 10740.
[37] L. L. G. Carrette, T. Morii, A. Madder, *Bioconjugate Chem.* **2013**, *24*, 2008 – 2014.
[38] K. Stevens, A. Madder, *Nucleosides Nucleotides Nucleic Acids* **2007**, *26*, 1359 – 1362.
[39] *IARC Monographs on the Evaluation of Carcinogenic Risks to Humans, Vol. 63*, Lyon, **1995**, pp. 393 – 407.
[40] N. Bakhiya, K. E. Appel, *Arch. Toxicol.* **2010**, *84*, 563 – 578.
[41] T. Kobayashi, J. Sugihara, S. Harigaya, *Drug Metab. Dispos.* **1987**, *15*, 877 – 881.
[42] M. C. Byrns, D. P. Predecki, L. A. Peterson, *Chem. Res. Toxicol.* **2002**, *15*, 373 – 379.
[43] A.-J. Cheng, J. C. Wang, M. W. Van Dyke, *Antisense Nucleic Acid Drug Dev.* **1998**, *8*, 215 – 225.
[44] O. Doluca, J. M. Withers, V. V. Filichev, *Chem. Rev.* **2013**, *113*, 3044 – 3083.
[45] L. E. Xodo, G. Manzini, F. Quadrifoglio, G. A. van der Marel, J. H. van Boom, *Nucleic Acids Res.* **1991**, *19*, 5625 – 5631.
[46] T. Kanamori, Y. Masaki, M. Mizuta, H. Tsunoda, A. Ohkubo, M. Sekine, K. Seio, *Org. Biomol. Chem.* **2012**, *10*, 1007 – 1013.
[47] A.-L. Guieysse, D. Praseuth, C. Giovannangeli, U. Asseline, C. Hélène, *J. Mol. Biol.* **2000**, *296*, 373 – 383.
[48] S. K. Swamynathan, A. Nambiar, R. V. Guntaka, *FASEB J.* **1998**, *12*, 515 – 522.
[49] Y. Ding, C. E. Lawrence, *Nucleic Acids Res.* **2001**, *29*, 1034 – 1046.
[50] S. A. Roberts, J. Sterling, C. Thompson, S. Harris, D. Mav, R. Shah, L. J. Klimczak, G. V. Kryukov, E. Malc, P. A. Mieczkowski, M. A. Resnick, D. A. Gordenin, *Mol. Cell* **2012**, *46*, 424 – 435.
[51] Z.-Y. Wang, T. F. Deuel, *Prog. Nucleic Acid Res. Mol. Biol.* **1996**, *55*, 227 – 244.
[52] S. Sasse-Dwight, J. D. Gralla, *J. Biol. Chem.* **1989**, *264*, 8074 – 8081.
[53] T. K. Prasad, V. Gopal, N. M. Rao, *FEBS Lett.* **2003**, *552*, 199 – 206.

Received: October 17, 2014
Published online on ■■ ■■, 0000

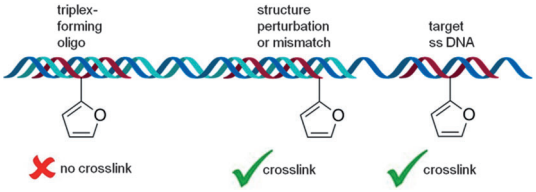

Exploiting perturbation: Furan-containing triplex-forming oligonucleotide probes are shown to selectively crosslink to perturbed sites in duplexes. Exposure of mixed single- and double-stranded sequences to furan-containing probes allows selective duplex crosslinking over triplex crosslinking.

*E. Gyssels, L. L. G. Carrette, E. Vercruysse, K. Stevens, A. Madder**

■■ – ■■

Triplex Crosslinking through Furan Oxidation Requires Perturbation of the Structured Triple-Helix